Thermochimica Acta, 149 (1989) 225–237
Elsevier Science Publishers B.V., Amsterdam – Printed in The Netherlands

A KINETIC STUDY OF HOLM OAK WOOD PYROLYSIS FROM DYNAMIC AND ISOTHERMAL TG EXPERIMENTS

T. CORDERO, F. GARCÍA and J.J. RODRÍGUEZ *
Department of Chemical Engineering, University of Malaga, 29071 Malaga (Spain)
(Received 2 January 1989)

ABSTRACT

The kinetics of holm oak wood thermal decomposition in a nitrogen atmosphere have been studied using dynamic and isothermal TG experiments. A number of different kinetic models are examined. Discrimination between the first order, second order and spherical symmetry boundary surface reaction models is difficult with the dynamic TG experiments. The isothermal weight loss curves obtained are best described by a first order rate equation.

INTRODUCTION

The pyrolysis of complex materials like wood and lignocellulosic biomass can be studied by focusing the attention on gaseous and condensable products [1–3] or by following the solid weight loss. This second method has been more widely used and is a useful practical approach when the main interest is with the solid product, as in charring, high temperature carbonization and activation. In these cases, the use of TG methods allows kinetic studies to be carried out by a simple and rapid experimental procedure. Nevertheless, a wide diversity of results have been reported in the literature [4,5]. Besides differences in the chemical compositions and physico-chemical structures of starting materials, certain experimental conditions such as sample amount, size and shape [5,6], thermal regime, temperature range and heating rate [7,8] have been found to affect significantly the results obtained. An important feature which has to be investigated in addition to the experimental conditions and in relation to them is the selection of a kinetic model. The importance of kinetic model discrimination as well as the method and the criteria used to determine the kinetics have been recognized by many authors dealing with the thermal decomposition of solids [9–12].

In this paper, we present results obtained for the thermal decomposition of holm oak wood under controlled experimental conditions (sample weight,

* To whom correspondence should be addressed.

particle size and heating rate) using different kinetic models. Dynamic TG experiments were carried out at several constant heating rates from 5 to 20 K min^{-1}. Isothermal experiments at different temperatures within the 220–340 °C range were also performed.

The kinetic models investigated include: first and second order homogeneous reaction; boundary surface reaction control with spherical symmetry; Avrami–Erofeev nuclei growth; and Prout–Tompkins branching nuclei. These models have been widely used in the literature for thermal decomposition of solid products [10–16]. However, in the case of cellulose and lignocellulosic biomass, the process has mostly been described by means of a first order reaction rate equation [4,5,7,17–20]. Kinetic order values other than 1, ranging from 0 to 3, have also been reported by some authors [4,10,21]. Fairbridge and coworkers have adopted a boundary surface reaction control model with cylindrical symmetry to explain the thermal decomposition of cellulose [22], and an integrated kinetic function resembling an Avrami–Erofeev model but with exponent 2 for pine bark and wood pyrolysis [23,24].

EXPERIMENTAL

TG curves were obtained using a Thermoflex Rigaku thermobalance. The initial sample weight was always adjusted to be close to 10 mg, and a 70 ml min^{-1} (STP) N_2 flow was continuously maintained. The raw material was powdered sawdust (65–80 mesh) from holm oak (*Quercus rotundifolia*). The sawdust was obtained from a single log of a tree more than 80 years old from Malaga, Spain, and was dried at 60 °C for 2 h before each TG experiment.

TG experiments were carried out in dynamic and isothermal conditions. In the first case, constant heating rates of 5, 7, 10, 12, 15 and 20 K min^{-1} were used; in the second, a preheating step at a constant heating rate of 7 K min^{-1} was followed by an isothermal stage which lasted 2 h. The temperatures studied in the isothermal experiments were 220, 240, 260, 275, 300, 325 and 340 °C.

KINETIC ANALYSIS OF TG DATA

The dynamic TG curves were analysed by the differential and integral methods. For the isothermal experiments, only the second of these methods was used, as simple analytical solutions are available for the rate expressions corresponding to the kinetic models investigated in this work.

The rate equation can be written as

$$d\alpha/dt = K(T)f(\alpha) \quad (1)$$

which in non-isothermal conditions becomes

$$d\alpha/dt = A \exp(-E/RT)f(\alpha) \quad (2)$$

where time and temperature are related by

$$T = T_0 + \beta t \quad (3)$$

β being the constant heating rate.

The conversion α for the dynamic experiments was defined as the actual weight loss (dry basis) referred to the total pyrolysable matter, i.e. the volatile matter of the starting material, which after six experimental determinations was taken as 84.5% of the initial sample weight, on a dry basis.

When using the differential method, a plot of $\ln[(d\alpha/dt)/f(\alpha)]$ vs. $1/T$ should give a straight line if the appropriate $f(\alpha)$ has been selected. The apparent activation energy and the pre-exponential factor are obtained from the slope and the intercept, respectively. The correlation coefficient r provides a first simple criterion for the comparison of different kinetic models, but it is not uncommon to obtain very similar r values from several models, which makes it difficult to discriminate between them. In addition to this criterion, the values of apparent activation energy obtained at different heating rates can also be used for model discrimination. If the experimental β values fall within a reasonably narrow range, so that it can be assumed that the chemistry of the process is not affected, then a model which describes the process well should lead to similar values of E at different heating rates.

In this work, the $d\alpha/dt$ values were obtained numerically using a cubic-spline function to describe the conversion–time curves.

Application of the integral method to dynamic TG experiments leads to

$$\int_0^\alpha \frac{d\alpha}{f(\alpha)} = g(\alpha) = A\int_0^t \exp[-E/R(T_0 + \beta t)]\, dt = \frac{A}{\beta}\int_{T_0}^T \exp(-E/RT)\, dT \quad (4)$$

Several approximate analytical solutions have been proposed for the RHS of this equation [25–27], but their validity is dependent on the temperature and the values of E. In the present work we have started from eqn. (2), which has been numerically integrated by the fourth order Runge–Kutta method. Iterations were carried out for each model and heating rate, varying A and E until the best possible fit between calculated and experimental $\alpha(t)$ values was obtained. Initial time was always fixed at the 180 °C temperature, since thermal decomposition was negligible up to this point. In each case, the starting E and A values for the iterations were those obtained from the differential method.

TABLE 1

Kinetic models investigated

Model	Symbol	$f(\alpha)$
First order reaction	F1	$1-\alpha$
Second order reaction	O2	$(1-\alpha)^2$
Boundary surface reaction, spherical symmetry	R3	$3(1-\alpha)^{2/3}$
Avrami–Erofeev nuclei growth	AE(1.5, 2, 3, 4)	$m(1-\alpha)[-\ln(1-\alpha)]^{1-1/m}$
Prout–Tompkins branching nuclei	PT	$\alpha(1-\alpha)$

Isothermal weight loss curves were analysed by the integral method, according to

$$\int_{\alpha_0}^{\alpha} \frac{d\alpha}{f(\alpha)} = g(\alpha) - g(\alpha_0) = kt \tag{5}$$

where α_0 corresponds to the conversion at the start of the isothermal stage (i.e. the preheating step conversion), and t refers to the isothermal time.

Thus, a plot of $g(\alpha)$ vs. t should yield a straight line with $g(\alpha_0)$ intercept when the appropriate kinetic model is used. The slope provides the apparent rate constant k.

Table 1 shows the kinetic models investigated in this work with their corresponding $f(\alpha)$ expressions.

RESULTS

Representative TG and DTG curves obtained for holm oak sawdust are presented in Fig. 1. The TG curve shows an initial weight loss attributed to moisture evaporation, followed by a plateau region up to 180 °C, a steep branch which extends up to 400 °C where the major weight loss takes place, and a final decay leading to a total weight loss close to 85%. The DTG curve exhibits a small maximum which is due to moisture loss, a shoulder between 295 and 340 °C, and a sharp maximum at 370 °C. The position of this maximum is fairly coincident with that observed by the authors for kraft lignin [28].

Dynamic experiments

From the TG curves we obtained conversion–time plots at the corresponding heating rates, which can be seen in Fig. 2. The numerical values of the derivative were calculated for at least 25 points in each curve, using a cubic-spline function as indicated above. From the plots of $\ln[(d\alpha/dt)/f(\alpha)]$

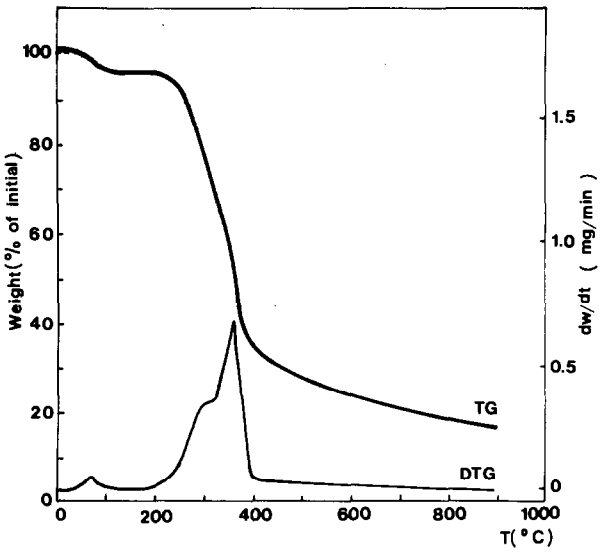

Fig. 1. TG and DTG curves for holm oak sawdust at $\beta = 10\,^{\circ}\mathrm{C\ min^{-1}}$.

vs. $1/T$, the apparent activation energy and the pre-exponential factor were determined for each kinetic model investigated, at each heating rate. The E values are presented in Table 2, where we have also included the mean value ($\bar{E}$) for each model, together with the standard (s) and mean relative (d) deviations.

The first order, second order and boundary surface reaction models provide very consistent results and complete discrimination between them

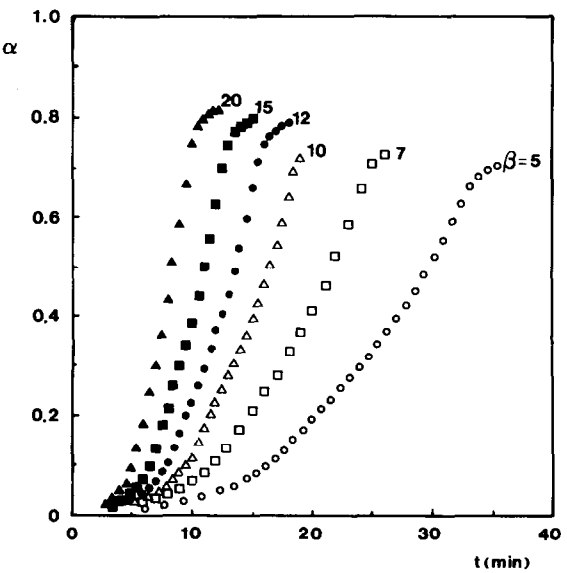

Fig. 2. Dynamic conversion–time curves.

TABLE 2

Apparent activation energy values (kJ mol^{-1}) from dynamic TG experiments using the differential method

β (°C min^{-1})	Model					
	F1	O2	R3	AE1.5	AE2	AE3
5	68.6	86.3	62.7	42.5	29.8	16.6
7	75.9	91.0	71.4	51.0	37.7	24.8
10	80.5	102.8	73.3	54.6	42.0	29.0
12	72.3	91.8	65.8	45.2	32.0	18.5
15	71.3	91.1	64.4	44.1	30.7	17.3
20	70.6	92.3	63.0	43.0	29.1	15.4
$\bar{E}$	73.2	92.5	66.8	46.7	33.6	20.3
s [a]	4.3	5.5	4.5	4.9	5.1	5.3
d (%) [b]	4.5	3.7	5.6	8.6	12.4	21.5

[a] $s = \left[\frac{\Sigma(E-\bar{E})^2}{n-1}\right]^{1/2}$

[b] $d = \frac{\Sigma(E-\bar{E})/\bar{E}}{n} \times 100.$

would be difficult. As can be seen, for the three models the activation energy values at different heating rates are fairly close, the O2 model giving the smallest mean relative deviation by a slight degree. In the three cases, the correlation coefficients resulting from the linear regression fits of $\ln[(d\alpha/dt)/f(\alpha)]$ vs. $1/T$ were higher than 0.99 at all the heating rates investigated. The Avrami–Erofeev model with $m = 1.5$ also led to good correlation coefficients, only slightly lower than those given above. Nevertheless, the relative deviations between the E values at different heating rates are somewhat higher. The remaining models give poorer results and the activation energy values seem less reasonable for reaction controlled kinetics. The AE4 and PT models have not been included in Table 2 as these provided highly dispersed data very far from linearity at all the heating rates investigated.

The results reported in Table 2 come from TG data falling within a temperature range varying from 220–345 °C for $\beta = 5$ °C min^{-1} to 235–380 °C for $\beta = 20$ °C min^{-1}. Outside this region, appreciable deviations were observed in the plots of $\ln[(d\alpha/dt(/f(\alpha)]$ vs. $1/T$. The reason may be that at lower and higher temperatures the pyrolysis process affects most predominantly the hemicellulose and the lignin, respectively, whereas in the intermediate range, i.e. the fitting range, the processes of thermal decomposition of hemicellulose, cellulose and lignin coexist [4].

The pre-exponential factor values showed higher relative deviations but these must be analysed in conjunction with the E values. A relation between

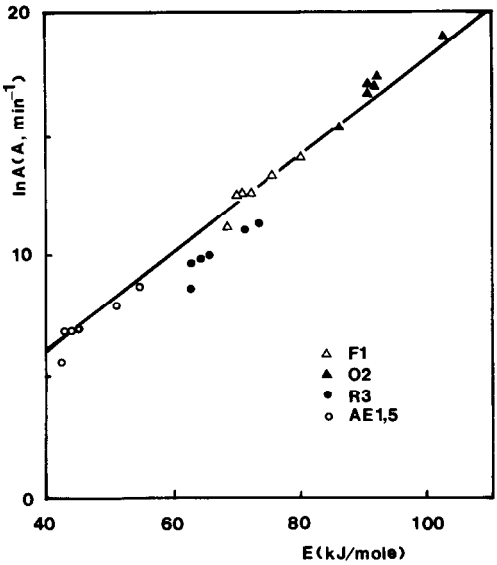

Fig. 3. A and E values from dynamic TG experiments using the differential method.

A and E called the kinetic compensation effect has been pointed out in the literature [29,30]. Figure 3 shows a plot of the values of ln A vs. the corresponding values of E given in Table 2. The straight line drawn corresponds to the equation

$$A = 0.156 \exp(0.2E) \tag{6}$$

which has been shown to apply to the kinetics of pyrolysis of wood and wood components [22,23]. In this equation, A is given in min^{-1} and E in kJ mol^{-1}.

As can be seen, except for the R3 model, the A and E values generally fall fairly close to the straight line representing eqn. (6), especially in the case of the data derived from the first order model.

The apparent activation energy values obtained by the integral method are presented in Table 3. The results are very similar to those reported in Table 2 for the differential method. Again, the A and E values fit the kinetic compensation effect given by eqn. (6) very well, as can be seen in Fig. 4. As before, discrimination between the first order, second order and boundary surface reaction models is difficult, as the three lead to very consistent results, showing fairly closely similar E values at different heating rates. The second order reaction model is again the one which gives the lowest mean relative deviation, by a slight degree, although the differences are not significant. A very close description of the experimental α–t curves was always obtained with these three models up to $\alpha = 0.8$, and increasing upward deviations were observed beyond this value. Residual analysis of the α–t (or T) data confirmed these observations and did not allow further discrimination.

TABLE 3

Apparent activation energy values (kJ mol^{-1}) from dynamic experiments using the integral method

β (°C min^{-1})	Model			
	F1	O2	R3	AE1.5
5	68.0	85.9	62.0	50.9
7	74.3	91.0	68.1	51.5
10	78.0	99.6	72.5	55.0
12	72.2	92.3	70.0	44.8
15	71.0	91.0	65.0	45.2
20	70.6	93.8	64.7	42.3
$\bar{E}$	72.4	92.3	67.1	48.3
s	3.4	4.5	3.9	4.9
d (%)	3.5	3.2	4.7	8.7

The results obtained using the remaining models were more consistent than those derived by the differential method, especially in the case of AE4 and PT models. Nevertheless, they performed less well than the other three models, and only the Avrami–Erofeev model with $m = 1.5$ provided a reasonably good description of the experimental α–t curves up to $\alpha = 0.3$, showing increasing deviations beyond this region.

Using the E and A values derived from the kinetic models investigated at each heating rate, the apparent kinetic constants resulting from the Arrhenius equation exhibited a systematic increase with β within the temperature

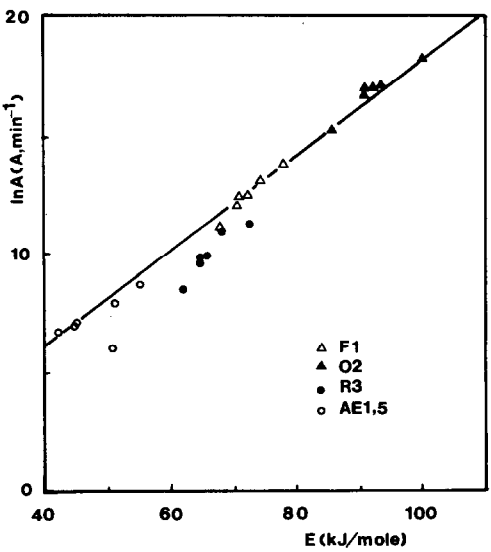

Fig. 4. A and E values from dynamic TG experiments using the integral method.

range investigated (with the single exception of the $\beta = 10\,^{\circ}\mathrm{C\ min^{-1}}$ values) in the case of the differential method. This was not observed for the integral method where, although the lowest values were always obtained at $\beta = 5\,^{\circ}\mathrm{C\ min^{-1}}$, at other heating rates the variations of the apparent kinetic constants did not show any relation to this variable.

Isothermal experiments

Figure 5 shows the weight loss curves obtained from the isothermal TG experiments. Significant differences were observed between the long term weight loss and the total volatile matter of the starting material, especially at temperatures lower than 300 °C. As we assume that pyrolysis is an irreversible process, to accomplish a correct kinetic analysis of the static TG curves conversion was referred in each case to the pyrolysable matter at the corresponding temperature, which was taken as the final weight loss after a 3 h period at the isothermal temperature. From the weight loss curves we obtained α–t data and $g(\alpha)$ vs. t plots for each kinetic model investigated. These plots are presented in Figs. 6 and 7 for the first order reaction model, which was the one which yielded the best fitting data at all the temperatures investigated. The remaining models showed a response quite a long way from linearity except in some particular cases, such as the R3 and AE1.5 models at 220 and 240 °C. The $g(\alpha)$ expression adopted by Fairbridge and Ross [24] for pine sawdust pyrolysis given by $g(\alpha) = [-\ln(1-\alpha)]^2$ was also checked, and was found to perform less well than the first order model in all cases.

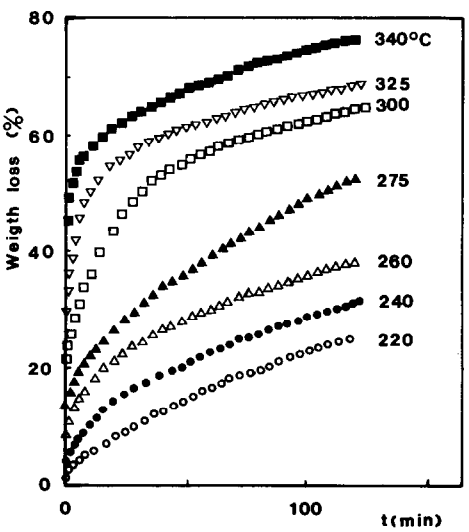

Fig. 5. Weight-loss curves from isothermal TG experiments.

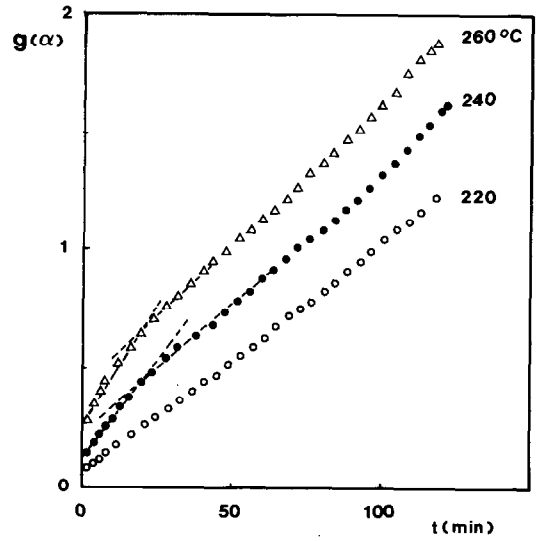

Fig. 6. Plots of $g(\alpha)$ vs. t for the first order reaction model from isothermal TG experiments at 220, 240 and 260 °C.

The plots in Figs. 6 and 7 indicate the existence of two linear regions, except at 220 and 270 °C where a single straight line can be adopted for the entire weight loss range covered. Because of the heterogeneous composition of wood, pyrolysis is a complex process involving consecutive and parallel thermal decomposition reactions. Focusing the attention on the three main wood components, hemicellulose decomposes first within the 200–260 °C

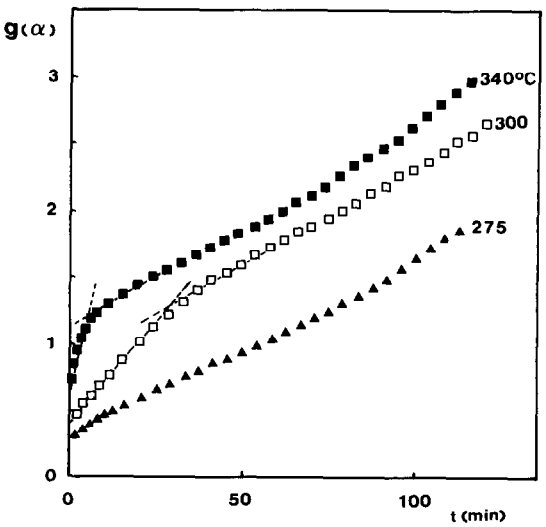

Fig. 7. Plots of $g(\alpha)$ vs. t for the first order reaction model from isothermal TG experiments at 275, 300 and 340 °C.

TABLE 4

First order apparent kinetic constants from isothermal and dynamic TG experiments

Temperature (°C)	K_H (10^3 min^{-1})	K_C (10^3 min^{-1})	K_{CL} (10^3 min^{-1})	$\bar{K}_{NI}$ (10^3 min^{-1})
220	9.8			6.7± 1.4
240	17.8	11.4		13.3± 2.8
260	31.0	12.4		25.1± 5.4
275		14.2		39.1± 8.6
300		31.4	15.2	78.2±17.9
325		68.9	12.2	147.5±35.4
340		95.1	16.9	210.7±52.2

temperature range, followed by cellulose from 240 °C to 350 °C and lignin throughout the 280–500 °C range [31]. These figures may undergo some variations but can be taken as highly indicative in a practical sense. Thus, at 220 °C pyrolysis principally affects hemicellulose, and a single apparent kinetic constant is obtained. At increasing temperatures cellulose decomposition becomes more significant, giving rise to a second linear region in the $g(\alpha)$ vs. t plots with a lower slope consistent with the lower reactivity of cellulose compared to that of hemicellulose [17,18]. The first linear branch becomes shorter as the temperature increases because more hemicellulose decomposes during the preheating stage. At 275 °C hemicellulose completion is achieved in the preheating step and a single straight line is obtained, corresponding basically to cellulose pyrolysis. At higher temperatures two linear regions are again noticeable. In the first, cellulose decomposition predominates, whereas in the second the contribution of lignin becomes increasingly significant as the temperature increases.

Table 4 gives the apparent kinetic constant values obtained at different temperatures for each of the above-mentioned regions. We have also included the mean K values obtained from the dynamic TG experiments by the integral method. The isothermal apparent kinetic constants are identified using the subscripts H, C and CL which refer, respectively, to the regions where hemicellulose, cellulose and cellulose plus lignin thermal decomposition predominates. For the non-isothermal experiment constants the subscript NI has been used.

The K_H values are consistent with the greater reactivity of hemicellulose whereas the K_{CL} values are indicative of the substantially lower reactivity of lignin compared to cellulose at the temperature investigated [32] (although the opposite has also been reported in the literature [17]). The apparently anomalous values of K_{CL} at 300 and 325 °C could be explained by a higher contribution of lignin pyrolysis in the CL region as temperature increases, giving rise to a lower overall reactivity which may not be compensated for by the kinetic effect of the temperature. With respect to K_C, it can be said

that the low temperature values (mainly 240 °C) are relatively high as compared with the remainder in an Arrhenius fashion. This is probably due to a significant contribution of hemicellulose in the C decomposition region at temperatures below 260 °C.

Orientative values can be obtained for the apparent activation energy and the pre-exponential factor within each of the three regions.

H region: $E = 63.3$ kJ mol^{-1}; $A = 4.5 \times 10^4$ min^{-1}

C region: $E = 83.5$ kJ mol^{-1}; $A = 1.2 \times 10^6$ min^{-1}

CL region: $E = 66.6$ kJ mol^{-1}; $A = 7.5 \times 10^3$ min^{-1}

For the C region we have excluded the 240 and 260 °C K_C values, and for the CL region only the 325 and 340 °C values have been taken.

A comparison between the K values derived from the isothermal and non-isothermal experiments shows that the second are about twice the K_C values, but when using the results obtained at the lowest heating rate investigated ($\beta = 5$ °C min^{-1}) instead of the mean K_{NI} values, the differences become substantially smaller. Nevertheless, this comparison should be viewed carefully, because the dynamic experiments lead to overall values for wood thermal decomposition and, on the other hand, conversion has been referred to different bases in dynamic and static experiments.

CONCLUSIONS

As a general conclusion, it can be pointed out that the first order reaction model provides a fairly good description of the kinetics of holm oak sawdust pyrolysis. The experimental TG curves in dynamic conditions at heating rates of between 5 and 20 °C min^{-1} are very well reproduced by means of this model using single overall values for the apparent activation energy and the pre-exponential factor within the major weight loss temperature range at each heating rate investigated. In the case of the isothermal experiments, the first order reaction is the best fitting model of all the kinetic expressions investigated, but to allow a close reproduction of the experimental weight loss curves two different values of the apparent kinetic constant must be used at all the temperatures investigated except at 220 and 275 °C.

ACKNOWLEDGEMENT

The authors wish to thank CAICYT for financial support for this research through Project AG-9/82 within the Agroenergetics Research and Development Programme.

REFERENCES

1 F. Shafizadeh and P.P.S. Chin, ACS Symp. Ser., 43 (1977) 57.
2 T. Thurner and U. Mann, Ind. Eng. Chem. Process Des. Dev., 20 (1981) 482.
3 T.R. Nunn, J.B. Howard, J.P. Longwell and W.A. Peters, Ind. Eng. Chem. Process Des. Dev., 24 (1985) 836.
4 A.F. Roberts, Combust. Flame, 14 (1970) 261.
5 H.A. Becker, A.M. Phillips and J. Keller, Combust. Flame, 58 (1984) 163.
6 P. Belleville, R. Capart and M. Gelus, Applied Energy, 16 (1984) 223.
7 R. Bilbao, J. Arauzo and A. Millera, Thermochim. Acta, 120 (1987) 121.
8 R. Bilbao, J. Arauzo and A. Millera, Thermochim. Acta, 120 (1987) 133.
9 L. Reich and S.S. Stivala, Thermochim. Acta, 58 (1982) 383.
10 P. O'Brien and S.D. Ross, Thermochim. Acta, 53 (1982) 195.
11 A.M. Gadalla, Thermochim. Acta, 74 (1984) 255.
12 A. Romero Salvador, E. García Calvo and J.M. Navarro, Thermochim. Acta, 87 (1985) 163.
13 J.M. Criado, F. González-García and J. Morales, Thermochim. Acta, 12 (1985) 337.
14 K.N. Ninan and C.G.R. Nair, Thermochim. Acta, 30 (1979) 25.
15 H. Tanaka, S. Ohshima, S. Ichiba and H. Negita, Thermochim. Acta, 48 (1981) 137.
16 T.P. Bagchi and P.K. Sen, Thermochim. Acta, 51 (1981) 175.
17 K. Akita, Rep. Fire Res. Inst. Japan, 9 (1956) 50.
18 A.J. Stam, Ind. Eng. Chem., 48 (1956) 413.
19 A. Murty, Combust. Flame, 18 (1972) 75.
20 R.R. Baker, J. Therm. Anal., 8 (1975) 163.
21 J.M. Baroah and V.D. Long, Fuel, 55 (1976) 116.
22 C. Fairbridge and R.A. Ross, J. Appl. Polym. Sci., 22 (1978) 497.
23 C. Fairbridge, R.A. Ross and P. Spooner, Wood Sci. Technol., 9 (1975) 257.
24 C. Fairbridge and R.A. Ross, Wood Sci. Technol., 12 (1978) 169.
25 A.W. Coats and J.P. Redfern, Nature, 201 (1964) 68.
26 V. Satava and F. Skvara, J. Am. Ceram. Soc., 52 (1969) 591.
27 T.V. Lee and S.R. Beck, AIChE J., 30 (1984) 517.
28 J.J. Rodríguez, T. Cordero and J. Rodríguez-Mirasol, Paper to be presented at the International Conference on Pyrolysis and Gasification, Luxembourg, May 1989.
29 A.K. Galwey, Adv. Catal., 26 (1977) 247.
30 D.J. Brown, Thermochim. Acta, 54 (1982) 377.
31 F.L. Browne, U.S. Dept. Agr. Forest Serv. Rep., 2136 (1958).
32 W.K. Tang, U.S. Dept. Agr. Forest Serv. Res. Paper FPL, 71 (1967).